Towards Long-Lasting Nanoscale Wireless Communications in the Terahertz Band for Biomedical Applications

Vittoria Musa[1,2], Giuseppe Piro[1,2(✉)], L. Alfredo Grieco[1,2], and Gennaro Boggia[1,2]

[1] Department of Electrical and Information Engineering, Politecnico di Bari, via Orabona 4, Bari, Italy
{vittoria.musa,giuseppe.piro,alfredo.grieco,gennaro.boggia}@poliba.it
[2] CNIT, Consorzio Nazionale Interuniversitario per le Telecomunicazioni, Parma, Italy

Abstract. During the last decade, the research on nanotechnology and wireless communications in the terahertz band supported the design of pioneering biomedical applications. To counteract the very scarce amount of energy available for nano-devices, a current challenge is to develop energy-aware and energy harvesting mechanisms enabling long-lasting communications at the nanoscale. Many contributions in this direction envisage exploiting piezoelectric nanogenerators to retrieve energy from external vibrations (i.e., the human heartbeat) and use it for transmission purposes. Indeed, in line with the recent scientific achievements in this context, this paper investigates a power control mechanism based on the feedback control theory. The control law is conceived for managing the communication in human tissues, where nano-devices are equipped with a piezoelectric nanogenerator and transmit information messages through electromagnetic waves in the terahertz band. The amount of energy spent to transmit an information message is dynamically tuned by a proportional controller in a closed-loop control scheme which simultaneously considers harvesting and discharging processes. The whole system is analytically described with a nonlinear state equation. As well, it is presented the acceptable range of values of the proportional gain guaranteeing technological constraints and its asymptotic stability. Finally, a numerical evaluation shows the behavior of the proposed approach in a conceivable biomedical scenario.

Keywords: Terahertz communications · Energy harvesting · Control law · Biomedical application

1 Introduction

The new frontier of nanotechnology is supporting the design of novel and advanced biomedical applications. In fact, nano-devices can be implanted,

ingested, or worn by humans in order to realize drug-delivering and advanced immune systems, biohybrid implant solutions, pervasive health monitoring, and genetic engineering [1]. The interaction among nano-devices can be enabled by nanoscale wireless communications in the terahertz band [11]. Since the communication process is energy-consuming, the usage of energy-aware and harvesting mechanisms is extremely important to achieve long-lasting communications at the nanoscale [6]. Many scientific contributions in this context assume to harvest energy from the external environment through piezoelectric nanogenerators [4,5,22] and, consequently, to use it in energy-aware communication protocols [2–4,12–14,18,20,21] (see Sect. 2). The idea to tune the transmission power based on the available energy budget has been recently investigated for diffusion-based molecular communications [15], but no works studied similar methodologies in nanoscale wireless communications and biomedical use cases.

To provide a step forward in this direction, this paper investigates a power control mechanism based on the feedback control theory. The control law is properly conceived for managing the communication in human tissues, where nanodevices are equipped with a piezoelectric nanogenerator and transmit information messages through electromagnetic waves in the terahertz band. Specifically, the amount of energy spent to transmit an information message is dynamically tuned by a proportional controller in a closed-loop control scheme which jointly considers harvesting and discharging processes. Here, the harvesting process is modeled as an ideal voltage source in series with a resistor and an ultra-nanocapacitor, while the discharging process is modeled through a current generator in parallel with the ultra-nanocapacitor. The resulting system is described by a nonlinear state equation where the voltage across the ultra-nanocapacitor and the resulting available energy represent the state variable and the feedback variable, respectively. Then, the acceptable range of values for the proportional gain is evaluated by considering 1) technological constraints, including transmission settings due to the Time Spread On-Off Keying (TS-OOK) modulation scheme and minimum energy requirements ensuring an effective communication in a stratified medium, and 2) the asymptotic stability of the system around the equilibrium point. Finally, a numerical analysis is performed to evaluate the impact of the proposed solution on the system behavior in conceivable biomedical scenarios, by considering different communication distances, frame sizes, and message generation statistics.

The rest of this work is organized as in what follows. Section 2 reviews the state of the art on energy harvesting and energy-aware schemes in the terahertz band. Section 3 presents the proposed approach. Section 4 discusses preliminary numerical results obtained in conceivable biomedical scenarios. Finally, Sect. 5 draws the conclusions of the work and summarizes future research activities.

2   Related Works

Traditional harvesting mechanisms (exploiting solar, thermal, and wind sources) are inefficient at the nanoscale. Thus, it is important to introduce new energy harvesting models, like those using mechanical and chemical sources [6,13].

Among the others, piezoelectric nanogenerators composed by lead zirconate titanate [16] or Zinc Oxide [22] nanowires, are widely considered promising solutions for retrieving energy at the nanoscale. Here, the vibrations or motions existing in the surrounding environment bent or compress the nanowires generating an electric current at their ends which charges an ultra-nanocapacitor [17].

Nowadays, several contributions already studied the usage of piezoelectric nanogenerators in nanoscale wireless communications. For example, [8] and [23] model the energy state of nano-devices through Markov chain, while jointly considering the energy harvesting rate and the energy consumption due to the communication process. The study presented in [24] theoretically investigates the achievable throughput of energy harvesting nanonetworks. Other contributions formulate energy-aware mechanisms at different levels of the protocol stack: the energy budget is used to define the time between two consecutive transmissions at the physical layer [4], to control data dissemination in a wireless nano-sensor network [18,20], and to properly manage the Media Access Control protocol [2,3,12–14,21].

At the time of this writing, and to the best of authors' knowledge, the information about the available energy budget has never been exploited for conceiving power control mechanisms in nanoscale wireless communication systems. In [15], the same authors of this paper propose a preliminary energy-aware transmission scheme for diffusion-based molecular communication that dynamically tunes (exploiting the control theory) the transmission power starting from the amount of available energy retrieved by a piezoelectric nanogenerator. This promising approach is applied herein in the context of nanoscale wireless communications enabling biomedical applications, while deeply taking into account the peculiarities of electromagnetic waves transmitted in the terahertz band and the propagation impairments registered in human tissues.

3   The Proposed Approach

This work considers a nano-device implanted in the human body and fed by a piezoelectric nanogenerator. It is able to collect biomedical information (e.g., the presence of sodium, glucose, other ions in blood, cholesterol, cancer biomarkers, and other infectious agents) and communicate them to a receiver positioned on the skin surface by means of electromagnetic waves in the terahertz band. Then, the obtained information can be transmitted to a remote device through traditional communication paradigms. The reference scenario is depicted in Fig. 1.

The main analytical symbols used in this paper are reported in Table 1.

3.1   Application Model and Transmission Scheme

At the physical layer, the nano-device sends messages of M bits by using the TS-OOK modulation scheme. These messages are generated according to a Poisson distribution with parameter λ. The duty cycle of the signal to transmit represents
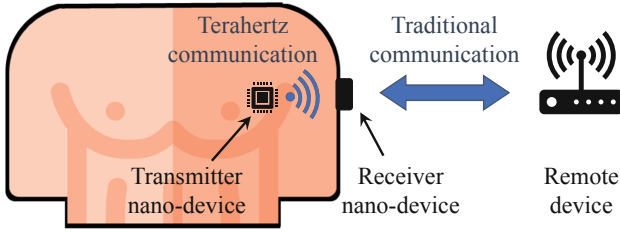
Fig. 1. The reference scenario.

Table 1. List of the main symbols used in this paper.

Symbol	Description
T_p, E_p	Time interval needed to transmit a pulse and resulting consumed energy
M	Number of bit per frame
λ	Average number of frames per second
σ, μ	Standard deviation and mean of the Gaussian pulse
d	Distance between transmitter and receiver nano-devices
f, f_m, f_M	Communication frequency, lower operative frequency, and higher operative frequency
$A_{abs}(f,d)$, $A_{spread}(f,d)$, $A(f,d)$	Absorption, spreading, and total path loss
$S(f)$, $N(f,d)$	Signal power spectral density and noise power spectral density
$\mathcal{C}(d)$	Upper bound of the channel capacity
$\delta(t)$, $\overline{\delta}$	Duty cycle of the signal to transmit and its average value
ρ	Occurrence probability of bit 1
v_h, $i_h(t)$, R_h	Generator voltage, generator current, and resistance of the circuit modeling the harvesting process
h_h	Amount of harvested energy per cycle
t_h	Time duration of the harvesting cycle
C_u	Capacitance of the ultra-nanocapacitor
$i_u(t)$	Current through the ultra-nanocapacitor
$i_d(t)$	Load current modeling the discharging process
g_p	Proportional gain of the controller
$V_u(t)$, $\dot{V}_u(t)$	Voltage across the ultra-nanocapacitor and its variation
E_0	Set point of the closed-loop control scheme
$E(t)$	Available energy budget at the ultra-nanocapacitor
E_{min}	Minimum amount of energy required to transmit bit 1
E_c	Amount of energy consumed per frame at the equilibrium
V_{eq}	Equilibrium point of the closed-loop control scheme

the ratio between the total amount of time spent to transmit the bits 1 of a frame and the frame duration itself. Thus, considering a probability of bit 1 equal to ρ, a pulse duration of T_p, and an average inter-arrival message time $1/\lambda$, the average duty cycle of the signal to transmit is equal to:

$$\overline{\delta} = \rho M T_p \lambda. \tag{1}$$

With TS-OOK, the bit 1 is encoded by means of a short pulse (i.e., $T_p = 100$ fs), and the bit 0 is represented by the silence. The pulse shape is modeled as a derivative of the Gaussian function with mean μ and standard deviation σ: $s(t) = (\sigma\sqrt{2\pi})^{-1}e^{-(t-\mu)^2/(2\sigma^2)}$ [7]. Considering the first derivative of that Gaussian function, the signal power spectral density of the pulse-based signal is:

$$S(f) = \left(\frac{E_p T_p}{\int_{f_m}^{f_M} (2\pi f)^2 e^{(-2\pi\sigma f)^2} df} \right) (2\pi f)^2 e^{(-2\pi\sigma f)^2} \tag{2}$$

where E_p, f_m, and f_M are the energy associated with a transmitted pulse, the lower operative frequency and the higher operative frequency, respectively.

3.2 Propagation Model and Channel Capacity

The propagation of the electromagnetic field in human tissues is modeled by considering a non-homogeneous and dispersive stratified medium, where each layer (stratum corneum, epidermis, dermis and fat) is defined by its dielectric properties and thickness [19]. The total path loss, $A(f,d)$, describes the total attenuation of the signal propagating across the human skin and is computed by summing the absorption path loss, due to the attenuation produced by the vibrations of the transmitted electromagnetic wave (i.e., $A_{abs}(f,d)|_{dB} = 10k(f)d\log e$, where $k(f)$ is the medium absorption coefficient), and the spreading path loss, due to the expansion of electromagnetic waves during the propagation (i.e., $A_{spread}(f,d)|_{dB} = 20\log(4\pi \int_{z_0}^{z} \frac{dz}{\lambda_g(f,d)})$, where z_0 is the reference section and λ_g is the wavelength of the plane wave propagating in the stratified medium [19]). The noise power spectral density is computed as $N(f,d) = k_B T_{eq}(f,d)$, where k_B is the Boltzmann constant and $T_{eq}(f,d)$ is the equivalent molecular noise temperature due to the molecular absorption.

To evaluate the Signal to Noise Ratio (SNR) and the resulting upper bound of the channel capacity, the total bandwidth B is divided into many narrow sub-bands lasting Δf, where the channel is non-selective. Then, the SNR for the i-th sub-band centered at the frequency f_i at a distance d, can be computed as: $SNR(f_i,d) = S(f_i)/(A(f_i,d)N(f_i,d))$. According to the Shannon theorem and considering (2), the upper bound of the channel capacity is affected by the pulse energy, E_p:

$$\mathcal{C}(d) = \sum_i \Delta f \log_2 \left[1 + SNR(f_i,d) \right] =$$

$$= \sum_i \Delta f \log_2 \left[1 + \frac{\left(\frac{E_p T_p}{\int_{f_m}^{f_M} (2\pi f)^2 e^{(-2\pi\sigma f)^2} df} \right)(2\pi f_i)^2 e^{(-2\pi\sigma f_i)^2}}{A(f_i,d)N(f_i,d)} \right]. \tag{3}$$

3.3   The Investigated Control Law

As depicted in Fig. 2(a), the nano-device retrieves energy from the vibrations in the surrounding environments by means of a piezoelectric nanogenerator composed by an array of Zinc Oxide nanowires [22], converts the alternating current in a direct one with a rectifier element, and stores the energy within an ultra-nanocapacitor. The retrieved energy is used to feed the communication processes.

The amount of energy available within the ultra-nanocapacitor is computed by jointly considering the harvesting and the discharging processes. According to [8,23], the harvesting process is modeled through an ideal voltage source, v_h, in series with a resistor, R_h, and the ultra-nanocapacitor, C_u. This source generates an amount of charge per cycle, h_h, every t_h seconds. Let $i_h(t)$, $i_u(t)$ and $V_u(t)$ be the generator current, the current passing through the ultra-nanocapacitor and the voltage across the ultra-nanocapacitor, respectively. The discharging process, instead, is modeled as a current source in parallel with the ultra-nanocapacitor with a load current $i_d(t)$. The resulting equivalent circuit describing the harvesting and discharging processes is shown in Fig. 2(b).

The methodology investigated in this paper allows a nano-device to dynamically tune the energy consumed for the transmission of a M-bits long frame starting from the amount of available energy with a feedback control scheme. Accordingly, the load current $i_d(t)$ is dynamically tuned with a proportional controller. The control law is designed with the aim of obtaining a positive value of $i_d(t)$, causing a positive energy consumption during the transmission of information messages. Accordingly, the proportional gain can only be greater than 0 (i.e., $g_p > 0$) and the energy budget available at the ultra-nanocapacitor, $E(t)$, is used as feedback variable. Furthermore, a null set point is considered (i.e., $E_0 = 0$), so that the load current, $i_d(t)$, is proportional to the available energy budget. The resulting feedback control system, depicted in Fig. 3, is analytically modeled by considering the voltage across the ultra-nanocapacitor, $V_u(t)$, as the state variable. Based on the procedure presented in [15], the time variation of the voltage across the ultra-nanocapacitor, $\dot{V}_u(t)$, caused by the aforementioned harvesting and discharging processes is modeled by the following state equation:

$$\dot{V}_u(t) = \frac{v_h}{R_h C_u} - \frac{V_u(t)}{R_h C_u} - \frac{g_p \delta(t) V_u(t)^2}{2}. \tag{4}$$

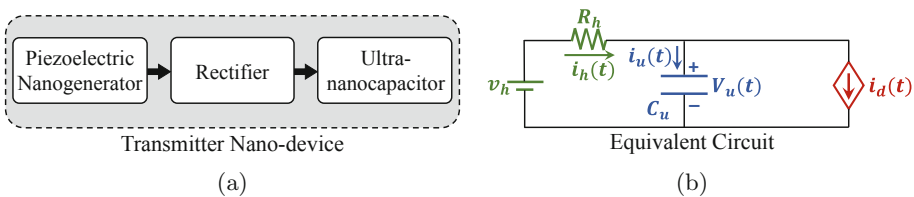Since $E(t) = C_u V_u(t)^2/2$, the resulting closed-loop control scheme is nonlinear.

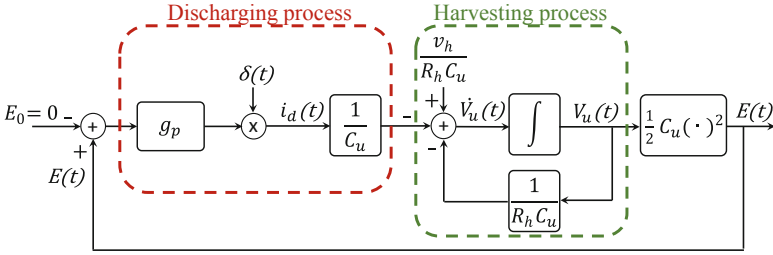Fig. 2. (a) Harvesting mechanism and (b) equivalent circuit modeling harvesting and discharging processes.

Fig. 3. The investigated closed-loop control scheme.

Equilibrium Point. After a transitory time, the system usually reaches one of the equilibrium points where it will remain for all future time. Analytically, for a continuous-time dynamical system, the equilibrium points are found by assuming a constant input (i.e., the average duty cycle of the signal to transmit, $\bar{\delta}$) and by imposing $\dot{V}_u(t) = 0$. Note that the equilibrium point should be a positive value. A negative equilibrium point, in fact, implies an inversion of the polarization of the voltage across the ultra-nanocapacitor, meaning that the load drains more current than the one generated by the harvesting process. Indeed, the only acceptable equilibrium point for the considered system is:

$$V_{eq} = \frac{-1 + \sqrt{1 + 2\bar{\delta}v_h g_p R_h C_u}}{\bar{\delta}g_p R_h C_u}. \tag{5}$$

Acceptable Value for the Proportional Gain. Besides the initial assumption on the proportional gain (i.e., $g_p > 0$), other technological constraints should be considered in order to evaluate the range of its acceptable values.

First, the equilibrium point in (5) must assume real values. Thus, the squared root and the denominator are set greater and different from zero, respectively:

$$1 + 2\bar{\delta}v_h g_p R_h C_u \geq 0 \text{ and } \bar{\delta}g_p R_h C_u \neq 0. \tag{6}$$

The analytical result of (6) states that $g_p \geq -1/2\bar{\delta}v_h R_h C_u$ and $g_p \neq 0$. Therefore, considering the initial assumption on the proportional gain (i.e., $g_p > 0$), this first condition is always verified.

Second, as highlighted in the derivation of the equilibrium point, it cannot be a negative value (i.e., $V_{eq} > 0$). This condition is always verified when $g_p > 0$.

Third, the equilibrium point cannot exceed the source voltage, v_h, that is $V_{eq} \leq v_h$. Accordingly:

$$V_{eq} = \frac{-1 + \sqrt{1 + 2\bar{\delta}v_h g_p R_h C_u}}{\bar{\delta}g_p R_h C_u} \leq v_h. \tag{7}$$

Also in this case, this condition is always satisfied when $g_p > 0$.

Finally, the fourth constraint states that the load current $i_d(t)$ and, in turns, the amount of consumed energy at the equilibrium, E_c, computed by the closed-loop control scheme should ensure the transmission of one packet entirely composed by 1-bits guaranteeing the target Shannon capacity level: $E_c = i_d(t)V_u(t)\lambda^{-1}|_{V_{eq},\bar{\delta}} \geq E_{min}$, where $E_{min} = ME_p$. Indeed, given that $i_d(t) = g_pC_u\delta(t)V_u(t)^2/2$, it comes that:

$$E_c = \frac{C_u\bar{\delta}g_pV_{eq}^3}{2\lambda} \geq E_{min}. \tag{8}$$

Analytically, (8) is verified if $-\frac{\sqrt{(v_h\lambda^{-1}(3E_{min}R_h-v_h^2\lambda^{-1}))^2-4E_{min}^3\lambda^{-1}R_h^3}}{E_{min}^2\bar{\delta}C_uR_h^3}$
$-\frac{v_h\lambda^{-1}(3E_{min}R_h-v_h^2\lambda^{-1})}{E_{min}^2\bar{\delta}C_uR_h^3} \leq g_p \leq \frac{\sqrt{(v_h\lambda^{-1}(3E_{min}R_h-v_h^2\lambda^{-1}))^2-4E_{min}^3\lambda^{-1}R_h^3}}{E_{min}^2\bar{\delta}C_uR_h^3}$
$-\frac{v_h\lambda^{-1}(3E_{min}R_h-v_h^2\lambda^{-1})}{E_{min}^2\bar{\delta}C_uR_h^3}$.

To sum up, among all the studied conditions, the fourth constraint determines both the upper and the lower bounds to the acceptable range of values of g_p.

Stability Analysis. The state equation in (4) can be linearized around the equilibrium point, V_{eq}, by using the Taylor series: $\dot{V}_u(t) = f(V_u(t), \delta(t)) \approx f(V_{eq}, \bar{\delta}) + \nabla f(V_{eq}, \bar{\delta}) \cdot [\mathcal{V}_u(t)\ \mathcal{D}(t)]^T$, where $f(V_{eq}, \bar{\delta}) = 0$ by definition, $\mathcal{V}_u(t) = V_u(t) - V_{eq}$ and $\mathcal{D}(t) = \delta(t) - \bar{\delta}$. Considering $\mathcal{V}_u(t)$ as the new state variable, the linearized state equation can be written as:

$$\dot{\mathcal{V}}_u(t) = \left.\frac{\partial f(V_u(t), \delta(t))}{\partial V_u(t)}\right|_{V_{eq},\bar{\delta}} \mathcal{V}_u(t) + \left.\frac{\partial f(V_u(t), \delta(t))}{\partial \delta(t)}\right|_{V_{eq},\bar{\delta}} \mathcal{D}(t) =$$
$$= \left(-\frac{1}{R_hC_u} - \bar{\delta}V_{eq}g_p\right)\mathcal{V}_u(t) - \frac{g_pV_{eq}^2}{2}\mathcal{D}(t). \tag{9}$$

The asymptotic stability around the equilibrium point of the linearized system in (9) is studied by posing the coefficient of $\mathcal{V}_u(t)$ less than 0 [10], that is: $-1/(R_hC_u) - \bar{\delta}V_{eq}g_p < 0$. By substituting (5) in this inequality, it comes $-\sqrt{1 + 2\bar{\delta}v_hg_pR_hC_u}/R_hC_u < 0$ which is always verified. Therefore, considering the initial assumption on the proportional gain (i.e., $g_p > 0$), it comes that the system having the state equation defined in (4) is asymptotically stable around V_{eq} for any $g_p > 0$.

4   Numerical Results

The following numerical analysis aims at evaluating the behavior of the investigated feedback control scheme in conceivable biomedical scenarios, while considering different communication distances, frame sizes, and message generation statistics. The results are obtained through Matlab scripts, modeling the system described in Sect. 3.

Table 2. Summary of simulation parameters.

Parameters	Values	References
T_p	100 fs	[8]
v_h	0.42 V	[8, 22]
C_u	9 nF	[5, 8, 17]
h_h	6 pC	[5, 8, 17]
t_h	1 s	[8, 22]
σ	0.15	[19]
f	[0.5 THz–1.5 THz]	[19]
M	40 bit–100 bit	[5, 8]
λ	10^{-2} frames/s–10^{-3} frames/s–10^{-4} frames/s	
d	3 mm–4 mm–5 mm	[8, 19]
$\mathcal{C}$	1 Mbps	[11]

Regarding the harvesting process, the proposed study considers the human heartbeat as energy source. According to [8,22], the time duration of the harvesting cycle and the generator voltage are equal to 1 s and 0.42 V, respectively. Given that the size of both piezoelectric nanogenerator and ultra-nanocapacitor strongly affect the capacitance of the ultra-nanocapacitor, C_u, and the amount of harvested energy per cycle, h_h, [5,8,17], when these sizes are equal to $1000\,\mu m^2$, reasonable values for C_u and h_h are 9 nF and 6 pC, respectively. The source resistor is set to $R_h = \frac{v_h t_h}{h_h}$ [8]. Starting from the propagation model presented in [19], the standard deviation of the pulse is set to $\sigma = 0.15$ and the communication frequency spans from 0.5 THz to 1.5 THz. To evaluate the impact of application settings on the system performance, the proposed analysis considers two frame sizes, that are $M = 40$ bit [5] and $M = 100$ bit [8], and an average number of frames per second, spanning from 10^{-2} frames/s to 10^{-4} frames/s. The values of system parameters used throughout the numerical evaluation are summarized in Table 2.

Figure 4 shows the upper bound of the channel capacity obtained according to (3) as a function of the communication distance and the pulse energy. Considering the target Shannon capacity equal to 1 Mbps, different communication distances equal to $d = 3$ mm, $d = 4$ mm, and $d = 5$ mm can be reached by setting the minimum required energy per pulse to $E_{min} = 10$ fJ, $E_{min} = 1$ pJ, and $E_{min} = 100$ pJ, respectively. These quantities are in line with the current state of the art [8,9,11].

Given the constraints presented in Sect. 3.3, Table 3 reports the range of acceptable values for the proportional gain considering the aforementioned parameter settings. It is important to note that the range of acceptable g_p drastically reduces with the frame size, the communication distance, and the average number of frames per second. Moreover, the configuration with communication distance equal to 4 mm, 100 bit per frame, and $\lambda = 10^{-2}$ frames/s has not
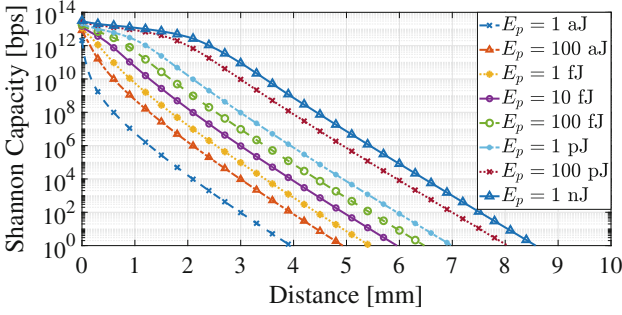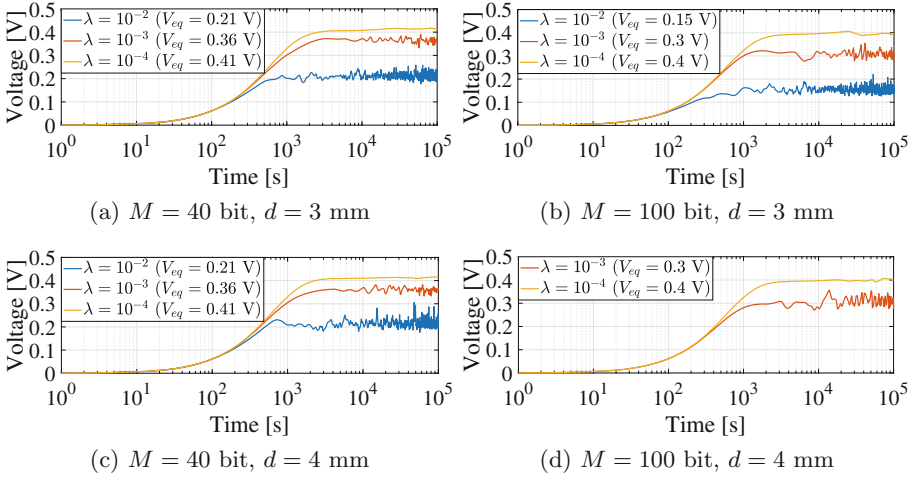
Fig. 4. Upper bound of the channel capacity.

(a) $M = 40$ bit, $d = 3$ mm

(b) $M = 100$ bit, $d = 3$ mm

(c) $M = 40$ bit, $d = 4$ mm

(d) $M = 100$ bit, $d = 4$ mm

Fig. 5. Variation of the state variable, $V_u(t)$, in the time domain.

Table 3. List of the minimum and maximum acceptable proportional gain values.

		$d = 3$ mm		$d = 4$ mm		$d = 5$ mm	
		$M = 40$ bit	$M = 100$ bit	$M = 40$ bit	$M = 100$ bit	$M = 40$ bit	$M = 100$ bit
$\lambda = 10^{-2}$ frames/s	g_{Pmin} [V^{-1}s^{-1}]	6.03×10^{8}	6.07×10^{8}	1.16×10^{11}	Unfeasible	Unfeasible	Unfeasible
	g_{Pmax} [V^{-1}s^{-1}]	1.5×10^{17}	9.48×10^{15}	7.74×10^{12}	Unfeasible	Unfeasible	Unfeasible
$\lambda = 10^{-3}$ frames/s	g_{Pmin} [V^{-1}s^{-1}]	6×10^{8}	6×10^{8}	6.3×10^{10}	6.8×10^{10}	Unfeasible	Unfeasible
	g_{Pmax} [V^{-1}s^{-1}]	1.5×10^{20}	9.6×10^{18}	1.43×10^{16}	8.46×10^{14}	Unfeasible	Unfeasible
$\lambda = 10^{-4}$ frames/s	g_{Pmin} [V^{-1}s^{-1}]	5.94×10^{8}	5.99×10^{8}	6.03×10^{10}	6.07×10^{10}	1.16×10^{13}	Unfeasible
	g_{Pmax} [V^{-1}s^{-1}]	1.5×10^{23}	9.6×10^{21}	1.5×10^{19}	9.5×10^{17}	7.74×10^{14}	Unfeasible

acceptable proportional gain values and it is unfeasible. As well, increasing of the communication distance to 5 mm makes unfeasible all the configurations, except the one for $M = 40$ bit and $\lambda = 10^{-2}$ frames/s. For the following analysis, only the communication distances equal to 3 mm and 4 mm are taken
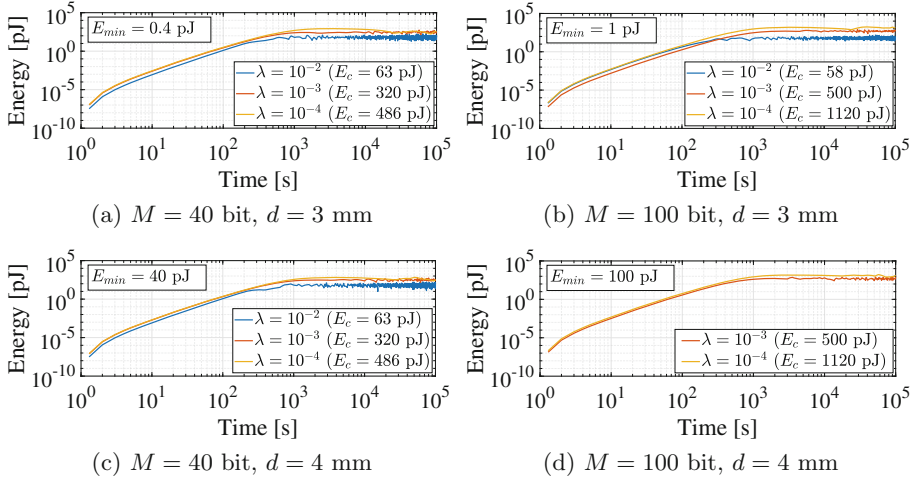
Fig. 6. Variation of the consumed energy in the time domain.

as example and a common intermediate value of g_p (i.e., $g_{pint} = 7.74 \times 10^{11}$ $V^{-1}s^{-1}$) is chosen starting from the resulting acceptable ranges.

Figure 5 depicts the variation of voltage across the ultra-nanocapacitor, $V_u(t)$, in the time domain as a function of the communication distance, d, the frame size, M, and the average number of frames per second, λ. Globally, the equilibrium point, V_{eq}, decreases when λ increases. In fact, given the frame size M and the distance between transmitter and receiver d, a higher λ implies a lower time interval between consecutive message generations. This way, the system has less time to retrieve energy, leading to a lower energy budget and a lower equilibrium point. At the same time, when the transmitter has to transmit a higher number of bit per frame, M, the energy budget decreases, thus reducing the value of the equilibrium point. It is worthwhile to note that, given the value of g_p, the communication distance does not affect the value of the equilibrium point.

The effect of λ, d, and M on the variation of the consumed energy in the time domain is shown in Fig. 6. First of all, the energy consumed at the equilibrium, E_c, is usually higher when M increases. Moreover, the decreasing of the average number of frames per second, λ, implies the increment of E_c. In fact, as demonstrated for the equilibrium point, higher values of λ correspond to lower energy budget. Thus, given the proportional gain g_p, the amount of energy consumed for the communication process is lower. Also in this case, when the g_p is fixed, the communication distance does not affect the value of the energy consumed at the equilibrium. On the other hand, the minimum amount of energy required to transmit a message entirely composed by 1-bits, E_{min}, obviously increases when the number of bit per frame and the communication distance increase. In any case, the amount of energy consumed at the equilibrium is higher than E_{min}.
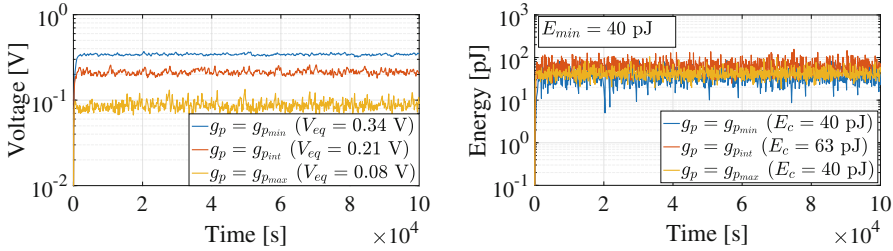
Fig. 7. Variation of (a) the state variable and (b) the consumed energy in the time domain during the transmission of a sequence of packets by considering three different acceptable values of g_p, $\lambda = 10^{-2}$ frames/s, $M = 40$ bit, and $d = 4$ mm.

As shown in Fig. 7(a), the voltage across the ultra-nanocapacitor and the amount of energy consumed for the packet transmission is also affected by the proportional gain, g_p. Given the average number of frames per second, the number of bit per frame and the communication distance, the equilibrium point increases when g_p decreases. In fact, lower values of g_p imply a decrement of the percentage of energy consumed for transmission purposes, allowing the system to reach higher equilibrium point. Combining the voltage across the ultra-nanocapacitor at the equilibrium and the value of the proportional gain, indeed, the maximum amount of energy is consumed when an intermediate value of g_p is used (see Fig. 7(b)).

5   Conclusion

This paper investigated a power control scheme for a nano-device fed by a piezo-electric nanogenerator and willing to communicate in human tissues through wireless communication in the terahertz band. After deriving the state equation of the resulting nonlinear system, the study of technological constraints and asymptotic stability provided the suitable range of values for the proportional gain. Finally, numerical examples showed the behavior of the proposed control approach in biomedical conceivable scenarios. This study demonstrated that the equilibrium point decreases when the inter-arrival message time decreases and the frame size increases, the resulting energy consumed at the equilibrium usually increases when the number of bit per frame and the inter-arrival message time increase, the increasing of the proportional gain implies the decreasing of the equilibrium point, and the maximum energy consumption is obtained when intermediate values of the proportional gain are used. Future research activities will investigate the effects of the conceived control law on the system performance, while jointly considering reception process and various network configurations.

References

1. Abbasi, O.H., et al.: Nano-communication for biomedical applications: a review on the state-of-the-art from physical layers to novel networking concepts. IEEE Access **4**, 3920–3935 (2016)
2. Akkari, N., et al.: Distributed timely throughput optimal scheduling for the internet of nano-things. IEEE Internet Things J. **3**(6), 1202–1212 (2016)
3. Alsheikh, R., Akkari, N., Fadel, E.: Grid based energy-aware MAC protocol for wireless nanosensor network. In: 2016 8th IFIP International Conference on New Technologies, Mobility and Security (NTMS), pp. 1–5 (2016)
4. Canovas-Carrasco, S., Garcia-Sanchez, A.J., Garcia-Haro, J.: A nanoscale communication network scheme and energy model for a human hand scenario. Nano Commun. Netw. **15**, 17–27 (2018)
5. Canovas-Carrasco, S., Garcia-Sanchez, A.J., Garcia-Haro, J.: On the nature of energy-feasible wireless nanosensor networks. Sensors **18**(5), 1356 (2018)
6. Chandrasekaran, S., et al.: Micro-scale to nano-scale generators for energy harvesting: self powered piezoelectric, triboelectric and hybrid devices. Phys. Rep. (2018)
7. Jornet, J.M., Akyildiz, I.F.: Channel modeling and capacity analysis for electromagnetic wireless nanonetworks in the terahertz band. IEEE Trans. Wireless Commun. **10**(10), 3211–3221 (2011)
8. Jornet, J.M., Akyildiz, I.F.: Joint energy harvesting and communication analysis for perpetual wireless nanosensor networks in the terahertz band. IEEE Trans. Nanotechnol. **11**(3), 570–580 (2012)
9. Jornet, J.M., Akyildiz, I.F.: Femtosecond-long pulse-based modulation for terahertz band communication in nanonetworks. IEEE Trans. Commun. **62**(5), 1742–1754 (2014)
10. Khalil, H.: Nonlinear Systems: Pearson New International Edition. Always Learning. Pearson Education Limited (2013)
11. Lemic, F., et al.: Survey on Terahertz Nanocommunication and Networking: A Top-Down Perspective, September 2019
12. Mohrehkesh, S., Weigle, M.C., Das, S.K.: DRIH-MAC: a distributed receiver-initiated harvesting-aware mac for nanonetworks. IEEE Trans. Mol. Biol. Multi-Scale Commun. **1**(1), 97–110 (2015)
13. Mohrehkesh, S., Weigle, M.C.: Optimizing energy consumption in terahertz band nanonetworks. IEEE J. Sel. Areas Commun. **32**(12), 2432–2441 (2014)
14. Mohrehkesh, S., Weigle, M.C.: RIH-MAC: receiver-initiated harvesting-aware MAC for nanonetworks. In: Proceedings of ACM The First Annual International Conference on Nanoscale Computing and Communication, pp. 1–9 (2014)
15. Musa, V., Piro, G., Grieco, L.A., Boggia, G.: A lean control theoretic approach to energy-harvesting in diffusion-based molecular communications. IEEE Commun. Lett. **24**(5), 981–985 (2020)
16. Niu, X.: High-performance PZT-based stretchable piezoelectric nanogenerator. ACS Sustain. Chem. Eng. **7**(1), 979–985 (2018)
17. Pech, D.: Ultrahigh-power micrometre-sized supercapacitors based on onion-like carbon. Nat. Nanotechnol. **5**(9), 651 (2010)
18. Pierobon, M., Jornet, J.M., Akkari, N., Almasri, S., Akyildiz, I.F.: A routing framework for energy harvesting wireless nanosensor networks in the terahertz band. Wireless Netw. **20**(5), 1169–1183 (2014)

19. Piro, G., Bia, P., Boggia, G., Caratelli, D., Grieco, L.A., Mescia, L.: Terahertz electromagnetic field propagation in human tissues: a study on communication capabilities. Nano Commun. Netw. **10**, 51–59 (2016)
20. Piro, G., Boggia, G., Grieco, L.A.: On the design of an energy-harvesting protocol stack for body area nano-NETworks. Nano Commun. Netw. **6**(2), 74–84 (2015)
21. Wang, P., Jornet, J.M., Malik, M.A., Akkari, N., Akyildiz, I.F.: Energy and spectrum-aware mac protocol for perpetual wireless nanosensor networks in the terahertz band. Ad Hoc Netw. **11**(8), 2541–2555 (2013)
22. Xu, S., Qin, Y., Xu, C., Wei, Y., Yang, R., Wang, Z.L.: Self-powered nanowire devices. Nat. Nanotechnol. **5**(5), 366 (2010)
23. Yao, X., Ma, D., Han, C.: ECP: a probing-based error control strategy for THz-based nanonetworks with energy harvesting. IEEE Access **7**, 25616–25626 (2019)
24. Yao, X.W., Wang, C.C., Wang, W.L., Jornet, J.M.: On the achievable throughput of energy-harvesting nanonetworks in the terahertz band. IEEE Sens. J. **18**(2), 902–912 (2017)